R. & M. No. 3464

MINISTRY OF TECHNOLOGY

AERONAUTICAL RESEARCH COUNCIL

# The Development of Injector Units for Jet-Lift Engine Simulation on Low-Speed-Tunnel Models

By M. N. Wood and J. B. W. Howard



LONDON: HER MAJESTY'S STATIONERY OFFICE
1967
PRICE 7s. 6d. NET

# The Development of Injector Units for Jet-Lift Engine Simulation on Low-Speed-Tunnel Models

By M. N. WOOD and J. B. W. HOWARD

*Reports and Memoranda No.* 3464*
*February*, 1965

*Summary.*

Small-scale injector units have been developed for providing the engine nacelles of V/STOL models, with both intake and exit flows. The primary energy supply was cold compressed air at pressure ratios up to 4:1. With the chosen injector arrangement, a stable and uniform exit velocity distribution was achieved, with a mean velocity of nearly 650 ft/sec, and almost 50 per cent of the jet efflux drawn in through the intake.

The requirements for engine simulation on model scale, and the capabilities and limitations of injector units for this application are discussed in an Appendix.

LIST OF CONTENTS



## 1. *Introduction.*

In all conditions where a V/STOL aircraft is partially jet-borne, experimental and theoretical studies[1,2] have shown that the basic aerodynamics are likely to be strongly affected by the presence of the lifting systems. Appreciable variations of pressure lift and large associated pitching moments may occur during the transition to and from cruise flight. Such interference effects can arise not only from the disturbances caused by the jet exit flows, but also from the intake flows, especially with configurations having upper surface intakes.

* Replaces R.A.E. Tech. Report 65020—A.R.C. 26897.

Considerable effort is being devoted to the study of these aerodynamic interference effects. There are extensive programmes of experimental research in low speed wind-tunnels, requiring much emphasis on the development of testing techniques[3]; but as yet, no completely adequate means are available for the full representation of the engine flows. When, as usual, only the jet efflux is represented, using cold compressed air at the correct engine pressure ratio to provide the scaled momentum flux, the main limitation concerns simply the problem of supplying sufficient compressed air to the model.

The practical representation of the intake flows is much more difficult. It is preferable to have separate control of the intake and exit flows, as this enables the aerodynamic interference effects to be studied independently. This involves the removal of the intake flow by means of a suction pump outside the tunnel, a technique which has been attempted with limited success at R.A.E.[4]. With more complex aircraft configurations, particularly those incorporating wing-mounted nacelles, it would not be possible in general to provide enough duct space inside the model to carry more than a small proportion of the air necessary for adequate intake simulation. Furthermore, the size of strut needed to carry the large intake flows from a complete model is liable to be intolerable from aerodynamic considerations.

An alternative approach to the problem is to use the principle of the injector pump to provide the intake and exit flows simultaneously, the most natural and convenient primary energy source being cold compressed air. The problems and limitations involved in the use of such injectors are discussed in the Appendix. It is shown that the ratios of intake to exit mass flows necessary for the simulation of the types of lift engine currently in use can only be achieved by accepting much reduced exit pressure ratios.

The problems of adequate engine flow representation became particularly acute in the design of the R.A.E. subsonic transport jet-nacelle research model[3]. On this model, vectored thrust and lift engine nacelles were mounted on the high-lift wing and it was appreciated that the intake flows could have a significant effect on the aerodynamics and must be represented at some stage. Moreover, with some multi-engined configurations, the quantities of compressed air which could be carried along the relatively small wing ducts would have provided unacceptably low jet velocities without some means of augmenting the exit mass flow.

Engine units incorporating injectors have been built for this model and the Report describes the short experimental programme leading to the final design of these units. The aim has been to produce nacelles with a stable and nearly uniform jet-efflux distribution of fairly high velocity*, together with appreciable intake flow. In practice, the aerodynamic interference effects measured with these nacelles will be compared with the interferences produced by similar nacelles with the same jet efflux but no intake flow, so that intake and jet effects can be separated. The emphasis on high exit velocities with a good distribution for research purposes has inevitably resulted in rather low intake mass-flow ratios, and it is not claimed that these units are suitable for complete engine flow simulation. However, with reasonable care in primary nozzle design, a good distribution of exit velocity can be produced with only a very short mixing tube, so that injectors become a practical proposition for engine simulation, assuming that some reduction in thrust loading is acceptable for model test purposes.

## 2. *Details of Injector Units and Test Procedure*

At the outset, the maximum nacelle size for a given jet exit area was specified by examination of typical engine installations. Two types of engine were considered, the small lightweight lift engine similar to the RB 162, and a larger propulsive engine with a single jet exit which could be rotated through large angles to give direct jet lift. No attempt was made in the time available to develop a representative vectored thrust unit, with intake flow as well as multiple swivelling nozzles, similar to the Pegasus engine used on the Hawker P1127. The development of such units may be desirable for specific aircraft model tests, but the additional complications likely to be encountered with injector units having multiple rather than single jet exits represent a real difficulty.

---

*High velocities were needed primarily to ensure adequate thrusts and aerodynamic loads relative to the sensitivity of the force balance.

The major problems to be faced in designing engine units for a small-scale model (1/20th-scale in this particular case) arise from the rather small size of the units and the short length available for the mixing of the primary and secondary airstreams inside the injector. With a simple injector consisting of a cylindrical mixing tube and a concentric circular primary nozzle, the optimum mixing-tube length for induction of secondary mass flow is between five and ten mixing-tube diameters, although even after this distance the velocity distribution is not uniform. If injectors are to be used for engine simulation, it is necessary for the mixing length to be reduced, say to the order of two mixing-tube diameters. This requires a fairly sophisticated primary nozzle configuration, designed to increase the mixing rate by augmenting the area of the mixing surface between the primary and secondary airstreams.

A simple unit for exploratory studies was constructed as shown in Fig. 1. It consisted basically of a cylindrical mixing tube surrounded by an annular reservoir supplying compressed air forward to the interchangeable primary nozzle units which could be inserted into the front of the mixing tube. Exit nozzles of contraction ratio 1·45 : 1, providing either zero or 90 deg deflection, could be fitted to the rear of the mixing tube. Consideration was restricted to primary nozzle configurations which could be manufactured on an even smaller scale. The various types of unit which were constructed are shown in Fig. 1. The first one consisted of a 'cartwheel' arrangement of eight spokes comprising elliptic tubes each with a trailing-edge blowing slot 0·08 inches wide. This arrangement was used first alone and then in conjunction with a peripheral blowing slot of width 0·03 inches, feeding primary air along the mixing tube wall. The second unit had the same peripheral blowing slot, used in conjunction with a central blowing arrangement. The third configuration had eight discrete blowing nozzles cut into the mixing-tube wall at an angle of 25 deg to the axis. The various ratios of mixing-tube cross-sectional area to primary-nozzle area are given in Fig. 2.

The primary mass flow was measured by means of a standard orifice plate in the compressed-air supply line. The bulk of the experimental work was carried out on a static rig, during the early part of 1962, and consisted of detailed traverses to measure the distribution of total and static pressure across the exit face of the injector. Hence, the exit velocity and also the mass flow and momentum flux at the exit of the injector could be calculated. Later, the complete injector unit was mounted in the No. 2 $11\frac{1}{2}$ ft$^2$ × $8\frac{1}{2}$ ft tunnel on the virtual-centre lower balance. The forces acting on the unit were measured for a range of primary pressures from 20 to 45 psig ($P_{01}/P_\infty$ = 2·35 to 4·0) and tunnel airspeeds from 0 to 200 ft/sec, with the axis of the unit at angles of 0, 15, 90 and 105 deg to the mainstream flow. When the unit was mounted so as to simulate a lift engine in forward flight the injector was surrounded by a large fairing to represent a lift pod. In all cases, a pitot-static rake was fitted inside the mixing tube to measure the effect of forward speed on the mass flow through the injector.

## 3. *Discussion of Results.*

### 3.1 *Exit Velocity Traverses on Static Rig.*

From the pitot and static traverses across the exit face of the injector, the exit velocity distributions were obtained. The local mass flow per unit area, $m$, was then derived and integrated over the exit area to give the total exit mass flow, and hence the mass ratio. The distribution of $m$ was very asymmetric in some cases, so that several traverses were then needed to determine the mass ratio $\left(\frac{\text{secondary mass flow}}{\text{primary mass flow}}\right)$ for any one condition. This was a tedious process and, in retrospect, it would have been preferable to measure the secondary flow directly. Only a limited number of pressure ratios were considered, but fortunately the mass ratio and the shape of the velocity distribution was not strongly dependent on pressure ratio for any particular geometric configuration.

Typical distributions of exit mass flow, $m$, are shown in Figs. 2 and 3, expressed in the form $\frac{m-m_1}{m_1}$, where $m_1$ is the primary mass flow per unit exit area. (N.B. for a symmetrical distribution $\int_0^1 \frac{m-m_1}{m_1}\left(\frac{r}{a}\right) d\left(\frac{r}{a}\right)$ = overall mass ratio.)

Distributions obtained across the exit of the mixing tube with no nozzle attached (Fig. 2) showed a very strong dependence on the primary nozzle configuration. Nozzle B, with 8 spokes but no peripheral jet, gave a very asymmetric distribution and there was some unsteadiness in the flow, illustrated by the hatched areas in Fig. 2. This was thought to be due to the separation of the flow from the wall caused by the adverse pressure gradient along the mixing tube, aggravated in this case by the short mixing length. Certainly the distribution was greatly improved when nozzle A was used, presumably because the additional peripheral jet served to provide boundary-layer control along the wall. The low mass ratio obtained with nozzle A was due to the small area ratio, which was chosen to give a high exit velocity. The effects of area ratio on performance are discussed in the Appendix.

Although the flow appeared to be steady with nozzle C (peripheral plus central jet, Fig. 2), it was extremely asymmetric. The central section of the primary flow was drawn away from the axis, probably due to some basic instability associated with the mixing process. Nozzle D gave a basically symmetrical distribution but there was some unsteadiness in the flow. No effort was made to ascertain whether this was due to wall boundary-layer separations or to the very powerful mixing processes which would occur with this configuration.

The contracting nozzle was fitted to the end of the mixing tube with the dual purpose of increasing the exit velocity and improving the distribution. Typical exit mass-flow distributions are given in Fig. 3 and can be compared directly with those in Fig. 2. Despite an inevitable increase in the pressure rise along the mixing tube, the contraction removed the flow unsteadiness and clearly improved the exit velocity distribution, though only at the expense of an appreciable reduction in overall mass-ratio.

Details of primary mass flow, overall mass ratio $\left(\text{i.e.}\dfrac{\text{secondary mass-flow}}{\text{primary mass-flow}}\right)$ and mean exit velocity are given in Table 1 for the more relevant configurations. No results are given for conditions where large flow asymmetries occurred, since the data would be potentially misleading.

Primary nozzle A, used in conjunction with the exit nozzle after the mixing tube, proved to be the most promising configuration, bearing in mind the requirement for a reasonably high and uniform exit velocity. With the primary pressure ratio at the design value of 3·65, the exit velocity varied from 670 ft/sec at the centre to 620 ft/sec just outside the wall boundary layer, with a mean value of about 640 ft/sec. The mass ratio was only 0·82, which would be quite inadequate for complete engine simulation (*see* Fig. 6). This could be improved slightly in practice with little or no reduction in exit velocity, by omitting the contraction after the mixing tube, increasing the primary nozzle area, and adjusting the balance of primary mass flow over the area of the mixing tube so as to improve the exit velocity distribution. However, Fig. 7 shows clearly that large increases in mass ratio could only be achieved by accepting further reductions in exit velocity.

The mixing-tube length was fixed at the maximum possible value which would fit into a specified nacelle and no attempt was made to study the effect of shortening the mixing length; inevitably, the adverse pressure gradient would then become more severe. However, velocity traverses at one mixing-tube diameter inside the mixing tube showed that, using primary nozzle A, most of the mixing had occurred by this station (Fig. 4) suggesting that primary-nozzle design should not become too complex if the mixing length was further reduced.

A realistic intake contour was used for most of these tests, but since this had only a small leading-edge radius (Fig. 1), additional measurements were made with a large bellmouth. However, any possible intake losses had only a minor effect on the mass-flow ratio, as would be expected with the low intake velocity (less than 320 ft/sec) of the present relatively inefficient injector unit.

### 3.2. *Force Measurements and Effects of Forward Speed*

The nacelle was mounted in the No. 2 $11\frac{1}{2}$ ft × $8\frac{1}{2}$ ft tunnel, the lift and drag forces being measured on the lower balance. Primary nozzle A in conjunction with an exit contraction ratio of 1·45:1 was the only configuration tested, mainly because the static exit-velocity traverses had shown that this gave the most promising results.

The static thrust was measured for a range of primary pressure ratios from 2·35 to 4·0, with jet deflection angles of 0 and 90 deg. The results are presented in Fig. 5, and can be compared directly with the theoretical primary-flow thrust, assuming isentropic expansion from the primary-supply pressure to atmosphere. The ratio of measured to theoretical thrust was approximately 0·88 for the basic nacelle with zero deflection, and 0·80 when the 90 deg turning vanes were fitted (*see* Fig. 5), whereas crude theoretical estimates using the form of analysis outlined in the Appendix suggest that the injector should provide about 20 per cent thrust augmentation relative to the theoretical primary thrust. The low experimental values would be due partly to the boundary-layer losses in the primary nozzle and the non-isentropic development of the primary flow, partly to skin-friction losses on the mixing tube wall, and, with the 90 deg deflection, to losses from the turning vanes.

Lift and drag measurements were also made at mainstream speeds up to 200 ft/sec with the axis of the nacelle at angles between 0 and 105 deg to the mainstream flow direction, to see if forward speed or incidence had any unpredictable effects on the performance of the injector. A theoretical estimate was made of forward-speed effects, using the method outlined in the Appendix, taking the free-stream dynamic head to be equivalent to an increase in $P_{o2}$, the intake stagnation pressure. The estimate showed that the increase in exit momentum would be more than counterbalanced by the intake momentum drag, and that between 0 and 200 ft/sec forward speed there would be a net drag rise of $1\frac{1}{4}$ lb and $2\frac{1}{2}$ lb at primary pressure ratios of 2·65 and 3·65 respectively.

Analysis of the experimental results was complicated by the difficulty which was experienced in defining the basic drag of the nacelle and the faired supporting strut. The rear of the nacelle was sharply boat-tailed (Fig. 1) and the external drag was presumably dependent on the ratio of exit to mainstream velocity. Furthermore, the drag of the supporting strut was found to be very sensitive to yaw angle. It was not found possible to obtain consistent and repeatable values for the basic drag and consequently the results could not be analysed in detail. Nevertheless, the drag increments were of the right order; at 200 ft/sec increments of 2 lb and $2\frac{3}{4}$ lb were measured (roughly 10 per cent of the static thrust in each case) at primary pressure ratios of 2·65 and 3·65 respectively, somewhat above the estimated values.

Force measurements were abandoned in favour of internal velocity traverses at a station two mixing-tube diameters downstream of the intake face. There was appreciable scatter in the results, probably because the traversing rake was only a short distance downstream of the primary nozzles. Nevertheless it was possible to detect variations in mass flow and velocity distribution in the mixing tube. As forward speed was increased from 0 to 200 ft/sec, the overall mass flow through the unit increased by approximately 3 and 10 per cent at pressure ratios of 3·65 and 2·65 respectively, compared with estimated increases of 3 and 7 per cent. The inclination to the mainstream of the axis of the injector had no detectable effect on either mass flow or velocity distribution with a primary pressure ratio of 3·65. In the most severe case examined, with a pressure ratio of 2·65 and an inclination of 90 deg, small reductions in total head (between 5 and 10 per cent of exit dynamic pressure) were noted on the upstream side of the mixing tube, causing a slight decrease in mass flow through the injector. This presumably occurred as a result of flow separations at the intake lip due to the relatively high mainstream speed.

In general, the injector was reasonably insensitive to external flow variations in the range of attitudes and velocity ratios relevant to engine simulation. It should be stressed, however, that this unit was not designed to achieve a high mass ratio. Larger performance variations are likely to occur with engine units designed to give large mass ratios (for more accurate engine representation) rather than high exit velocities, as in the present case. Such units would inevitably be operating under conditions where small changes in intake stagnation pressure and aerodynamic back pressures would have large effects on the mass ratio and thrust. Very careful calibrations would then be needed to define the performance of such injectors throughout the working range, in order to isolate the aerodynamic interference effects. In extreme conditions this could well prove impracticable, in which case the forces on the engine units would need to be measured independently of the main aerodynamic loads, by mounting the injector units either from the model *via* strain-gauge balances or from a completely separate external balance[3].

## 4. *Concluding Remarks*

A small, compact injector unit driven by cold compressed air has been developed to provide, within the size and shape of a typical model-scale engine nacelle, a uniform high-velocity jet efflux with appreciable induced intake flow. The jet velocity at all points outside the nozzle boundary layer is within 5 per cent of the mean value of 640 ft/sec at the design supply pressure-ratio of 3·65. Slightly less than 50 per cent of the jet efflux is drawn through the intake by the inducing action of the primary air. This mass ratio, though adequate for the research studies for which the unit was developed, is not sufficient for complete engine simulation, mainly because the design concentrated on achieving a high exit velocity. The mass ratio could certainly be increased if lower exit velocities were acceptable, and with careful design, engine units should be able to operate satisfactorily with even shorter mixing lengths.

The performance of the present unit is not very sensitive to changes in the external flow. However, with more efficient injector units, designed to give more representative intake mass-flow rates, increased sensitivity may be found, and this could present an appreciable design and calibration problem.

---

# APPENDIX

## *A Consideration of the Requirements for Engine Simulation*

When considering the simulation of engines on model scale it is important to decide which features of the engine flow will have the most significant effects on the external aerodynamics. The shape, size and position of the intakes and the intake mass flow, together with the shape, size and position of the jet exits and the jet temperature, pressure ratio, mass flow, momentum flux and velocity distribution are all factors which could affect the external flow field. Consideration should also be given to possible Reynolds number effects.

The intake flow can perhaps most usefully be represented by sinks suitably distsibuted over the intake face. At appreciable distances from the intake, the induced velocity will depend primarily on the position of the intake and the intake mass flow, i.e. overall sink strength, rather than on the actual sink distribution. Thus the overall effects of the intake may not depend greatly on the precise size and shape, except in conditions where the intake flow is liable to affect directly the type of flow over adjacent aerodynamic surfaces.

On the other hand, experiments on a single circular jet exhausting from a plane wall into a mainstream flow[2] have shown that the size of the jet as well as the exit momentum is an important factor in determining the interference from the exit flows. It thus seems sensible at this stage to insist that the exit geometry should be carefully reproduced at model scale. An extension of the work of Ref. 2 has also suggested that jet temperature, pressure ratio and velocity are in themselves relatively unimportant. Little is known as yet about the effects of exit velocity distribution or jet Reynolds number.

Thus, the absolute minimum requirements for engine simulation on model scale appear to be:

(1) scaled exit geometry

(2) correct exit-momentum coefficient

(3) correct intake position but not necessarily exact representation of intake geometry

(4) correct intake mass-flow coefficient.

Other features of the engine flow would seem in general to be of secondary, though not necessarily negligible, importance.

In considering the simulation of engines using injector units driven by cold compressed air, several limitations must be faced at the outset. The exit flow will be cold and, in practice, it will prove impossible to achieve the correct exit pressure ratio. In addition, as shown in the subsequent analysis, the ratio of exit to intake mass flow will be considerably greater than unity, whereas it is only about 1·02 for a typical turbojet engine. However, assuming that these are not considered unacceptable limitations, it is worth investigating what is involved in matching the coefficients of intake mass flow and exit momentum flux.

In the following, the symbol $Q$ represents mass flow, $u$ velocity, $\rho$ air density, $T$ the absolute temperature, $S$ wing area, $A_j$ jet exit area; the suffix '$i$' denotes intake, '$j$' exit, '$\infty$' free stream, '$m$' model, and '$f$' full scale.

Thus, the representation of intake mass-flow coefficient and exit momentum coefficient implies

$$\frac{Q_{if}}{Q_{im}} = \frac{\rho_{\infty f} u_{\infty f} S_f}{\rho_{\infty m} u_{\infty m} S_m} \tag{1}$$

and

$$\frac{Q_{jf} u_{jf}}{Q_{jm} u_{jm}} = \frac{\frac{1}{2}\rho_{\infty f} u_{\infty f}^2 S_f}{\frac{1}{2}\rho_{\infty m} u_{\infty m}^2 S_m} = \frac{u_{\infty f}^2 S_f}{u_{\infty m}^2 S_m} \tag{2}$$

for an atmospheric tunnel.

Equally

$$\frac{Q_{jf} u_{jf}}{Q_{jm} u_{jm}} = \frac{\rho_{jf} u_{jf} A_{jf}}{\rho_{jm} u_{jm} A_{jm}} \frac{u_{jf}}{u_{jm}} \simeq \frac{T_{jm}}{T_{jf}} \frac{u_{jf}^2}{u_{jm}^2} \frac{A_{jf}}{A_{jm}}. \tag{3}$$

For scaled jet areas $\frac{S_f}{S_m} = \frac{A_{jf}}{A_{jm}}$, so that comparing (2), (3)

$$\frac{u_{\infty f}^2}{u_{\infty m}^2} \simeq \frac{T_{jm}}{T_{jf}} \frac{u_{jf}^2}{u_{jm}^2}. \tag{4}$$

From (1) and (2)

$$\frac{Q_{jm}}{Q_{im}} = \frac{Q_{jf}}{Q_{if}} \frac{u_{jf}}{u_{jm}} \frac{u_{\infty m}}{u_{\infty f}}$$

$$\simeq \frac{Q_{jf}}{Q_{if}} \sqrt{\frac{T_{jf}}{T_{jm}}} \text{ from (4)}$$

$$\simeq \sqrt{\frac{T_{jf}}{T_{jm}}} = F$$

since

$$Q_{jf} \simeq Q_{if}.$$

The exact value of $\frac{Q_{jm}}{Q_{im}}$ requires knowledge of the fuel-air mass ratio for the engine, and also the relationship between $\rho_j$ and $T_j$, which is a function of exit Mach number and may be different in the two cases. However, the relationship $\frac{Q_{jm}}{Q_{im}} = F$ is unlikely to be in error by more than about 5 per cent.

The significance of this relationship is that $F$ is greater than unity since the model flows are here assumed to be relatively cold, below 300 deg K, whereas the full-scale exit temperature may be anything up to 800 or 900 K, depending on the type of engine being considered. The mass ratio is usually defined as

$$\frac{\text{induced mass flow}}{\text{primary mass flow}} = \frac{Q_i}{Q_j - Q_i} = \frac{1}{F-1}$$

and in Fig. 6 this relationship is used to provide a curve of required model mass ratio against desired engine exit temperature, assuming the model jet to be at 288 deg K.

These mass ratios do not seem large in themselves when compared with the values associated with the more usual applications of injectors. For full engine representation, however, the mass ratio must be achieved with as high an exit velocity as possible, and this, combined with the requirement of short mixing lengths, presents an appreciable design problem. Very little experimental data on injector performance exists in the region of interest for the present application and, at this stage, theoretical curves give the best guide to the likely problems and limitations. A method of presentation suggested in some unpublished work by Lopez of B.A.C. (Warton) shows very clearly the importance of the various parameters. Some results from this analysis, which is based on considerations of mixing at constant area, are reproduced in Fig. 7. The notation is as follows :

$A_R$ area-ratio $= \dfrac{\text{Area at end of mixing tube}}{\text{Primary nozzle throat area}}$

$P_{o1}$ primary stagnation pressure

$P_{o2}$ stagnation pressure of induced flow

$P_4$ ambient static pressure at end of mixing tube

$P_\infty$ ambient static pressure of external mainstream flow

$M_3''$ Mach number of induced flow at position of primary nozzle throat.

The mass ratio is found to be a function of only two parameters $\left(\frac{P_{o1}}{P_4}\right)\left(\frac{1}{A_R}\right)$ and $\left(\frac{A_R-1}{A_R}\right)\left(\frac{P_{o2}}{P_4}\right)$, and can conveniently be plotted against the primary parameter $\left(\frac{P_{o1}}{P_4}\right)\left(\frac{1}{A_R}\right)$ for a range of values of secondary parameter $\left(\frac{A_R-1}{A_R}\right)\left(\frac{P_{o2}}{P_4}\right)$. Curves of secondary Mach number $M_3''$ are also presented; for the area and pressure ratios relevant to the present discussion, analysis shows that $M_3''$ is closely similar to the Mach number at the end of the mixing tube.

It will be seen that each mass-ratio curve shows a maximum value and hence there is a theoretical optimum design point for any specified value of the secondary parameter. If the primary parameter $\left(\frac{P_{o1}}{P_4}\right)\left(\frac{1}{A_R}\right)$ is above its optimum value, then an increase in the area-ratio $A_R$ will give a twofold gain in mass-flow ratio since the primary parameter will then decrease while the secondary parameter

$\left(\frac{A_R-1}{A_R}\right)\left(\frac{P_{o2}}{P_4}\right)$ will increase. Again, an increase in supply pressure has a favourable effect on performance since it permits an increase in $A_R$ for a given primary parameter, which in turn increases the secondary parameter and hence the mass ratio. In practice, such gains would tend to be offset somewhat by the increased stressing problems arising from the use of higher pressures.

The ratio $P_{o2}/P_4$ which appears in the secondary parameter is affected by both intake and exit conditions. $P_4$ will be a function of the geometry between the end of the mixing tube and the jet exit and $P_{o2}$ will depend on the free-stream dynamic pressure and the intake efficiency.

It must be realised that these are theoretical curves and that viscous effects will reduce the performance. Much more experimental data will be needed in order to determine the extent of the reduction throughout the range of current interest. The existing evidence suggests that viscous effects reduce the performance by about 10 per cent and that the optimum performance is achieved with a higher value of primary parameter than that defined theoretically. These viscous effects are not excessive so the theoretical curves form a useful basis for injector design.

In designing an injector for any prescribed application, the maximum available supply pressure would be known, and the required mass ratio effectively would be specified by the engine jet-pipe temperature (Fig. 6). The area-ratio $A_R$ is then selected by an iterative process to yield as high a value of $M_3''$ as possible. A comparison between Figs. 6 and 7 shows clearly the most severe limitation of injectors for engine simulation. The required mass ratio rises sharply as the engine temperature decreases and Fig. 7 shows that this can only be obtained by accepting a reduction in $M_3''$ and, in turn, the exit velocity.

The exit velocity distribution cannot be controlled by means of internal baffles or gauzes, as in the case of models using compressed air for jet simulation only, since these would cause unacceptable reductions in the intake mass flow. The distribution must be adjusted instead by careful primary nozzle design. This problem is particularly severe with multi-nozzle arrangements, similar to the Pegasus vectored thrust engine, where the correct balance of mass flow to the various nozzles must be achieved and the flow deflected through large angles. There is a temptation to increase the mixing tube diameter so as to reduce the internal velocities, and then to include a contraction in the jet nozzle so as to improve the exit velocity distribution. However, this effectively reduces the mixing tube length, complicating the primary nozzle design still further. Furthermore, the secondary parameter is reduced since $P_4$ is increased, especially with high exit velocities, thus reducing the mass ratio.

The design of injector units for engine simulation therefore becomes a compromise between the conflicting requirements of high mass ratio, high exit velocity and controlled velocity distribution. A great deal more experimental work will be needed to provide a firm foundation for the detailed design of small, highly efficient engine units.

TABLE 1

*Static Injector Performance*

| Primary | Exit | Primary | Primary mass flow (lb/sec) | Mass ratio secondary primary | Mean exit velocity (ft/sec) |
|---|---|---|---|---|---|
| A | On | 3·0 | 0·63 | 0·95 | 565 |
| A | On | 3·65 | 0·78 | 0·82 | 640 |
| A | On | 4·0 | 0·84 | 0·82 | 690 |
| A | Off | 3·65 | 0·78 | 1·24 | 580 |
| B | On | 3·0 | 0·44 | 1·41 | 515 |
| B | On | 3·65 | 0·55 | 1·24 | 570 |
| C | On | 3·65 | 0·48 | 1·17 | 490 |
| D | On | 3·0 | 0·46 | 1·22 | 480 |
| D | On | 3·65 | 0·56 | 0·92 | 520 |
| D | Off | 3·65 | 0·56 | 1·00 | 375 |

## LIST OF SYMBOLS

| | |
|---|---|
| $a$ | Radius of jet exit |
| $A_j$ | Jet exit area $= \pi a^2$ |
| $A_R$ | Area ratio $= \dfrac{\text{cross-sectional area of mixing tube}}{\text{primary nozzle throat area}}$ |
| $m$ | Total injector mass flow/unit exit area |
| $m_1$ | Primary mass flow/unit exit area |
| $M_3''$ | Mach number of secondary flow at position of primary nozzle |
| $P_{01}$ | Primary supply pressure |
| $P_{02}$ | Stagnation pressure of secondary flow |
| $P_4$ | Ambient static pressure at end of mixing tube |
| $P_\infty$ | Mainstream ambient static pressure |
| $Q$ | Mass flow |
| $r$ | Radial distance from axis of injector |
| $S$ | Wing area |
| $T$ | Temperature |
| $u$ | Velocity |
| $\rho$ | Density |

*Suffices*

| | | |
|---|---|---|
| $i$ | Intake | Conditions |
| $j$ | Jet exit | |
| $f$ | full scale | |
| $m$ | Model scale | |
| $o$ | Stagnation | |
| $\infty$ | Mainstream | |

## REFERENCES


| *No.* | *Author(s)* | *Title, etc.* |
|---|---|---|
| 1 | J. Williams . . . . . | Comments on some recent basic research on V/STOL aerodynamics. A.R.C. 23693. November, 1961. |
| 2 | L. J. S. Bradbury and M. N. Wood | The static pressure distribution around a circular jet exhausting normally from a plane wall into an airstream. A.R.C. C.P. 822. August, 1964. |
| 3 | J. Williams and S. F. J. Butler | Further developments in low-speed wind-tunnel techniques for V/STOL and high-lift model testing. A.R.C. 25849, January, 1964. |
| 4 | M. N. Wood . . . . | Unpublished M.O.A. Report. |

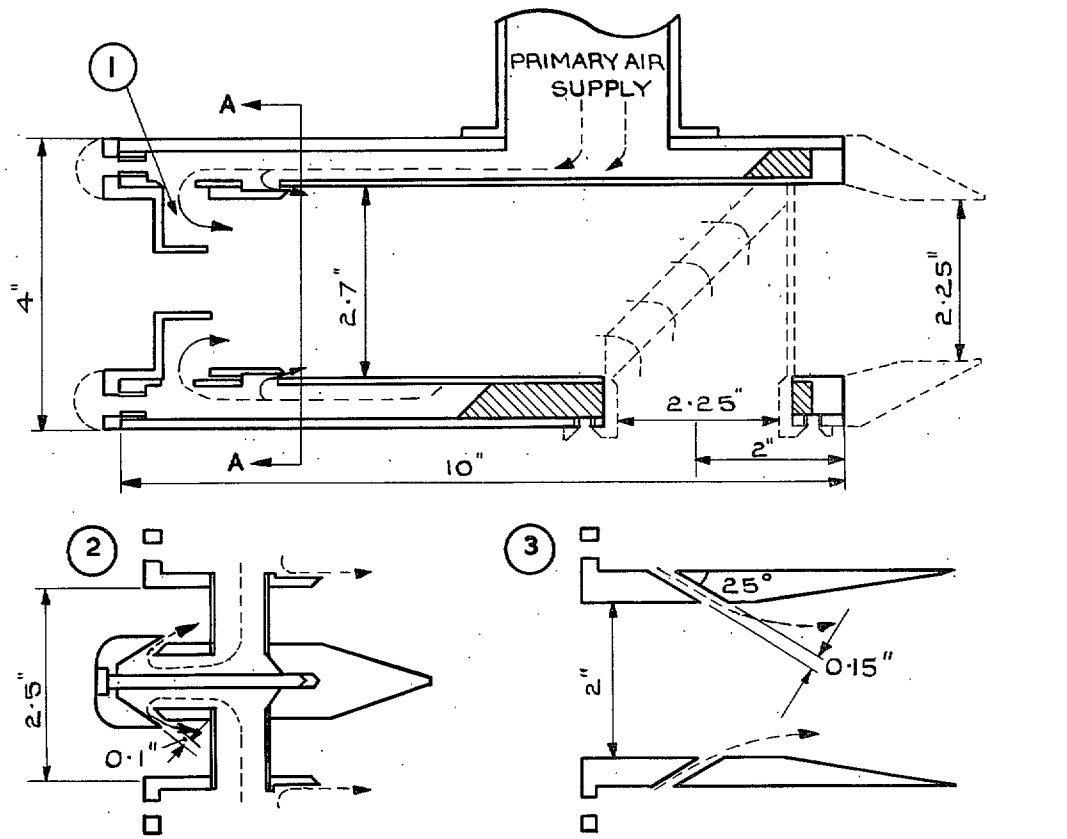


SECTIONS ON CENTRE LINE OF NACELLE AND PRIMARY NOZZLES

(1) CARTWHEEL (2) CONCENTRIC RING AND (3) DIVIDED RING NOZZLES

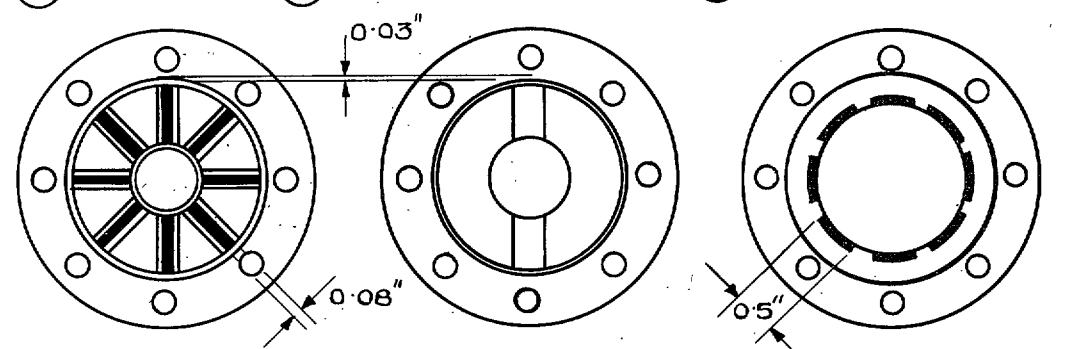


VIEW OF CARTWHEEL NOZZLE FROM A–A

SIMILAR VIEWS OF CONCENTRIC AND DIVIDED RING NOZZLES

FIG. 1. Details of injector units.

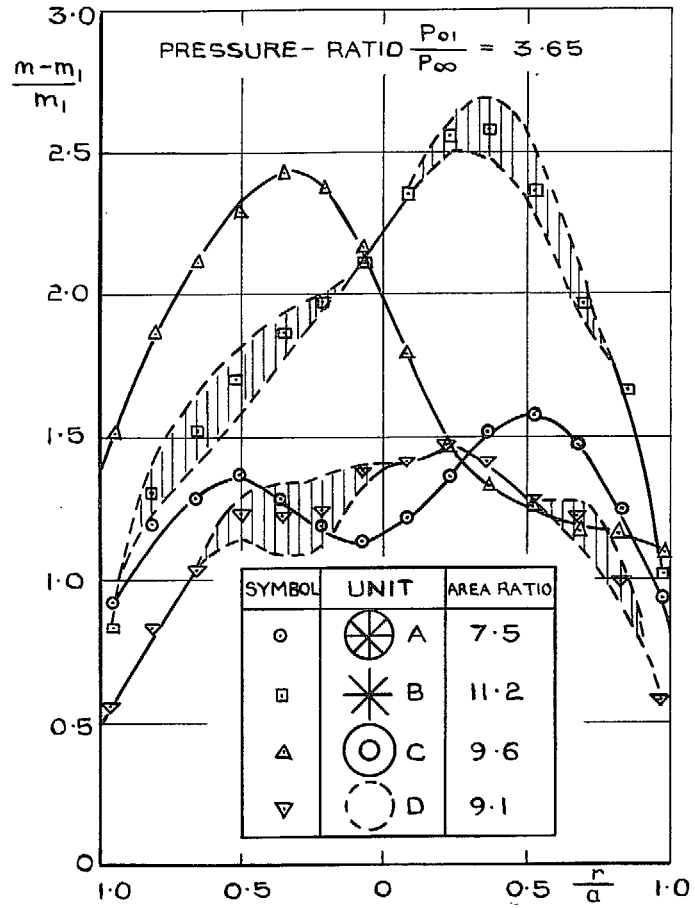


FIG. 2. Typical mass-ratio distributions at end of mixing tube. No exit nozzle.

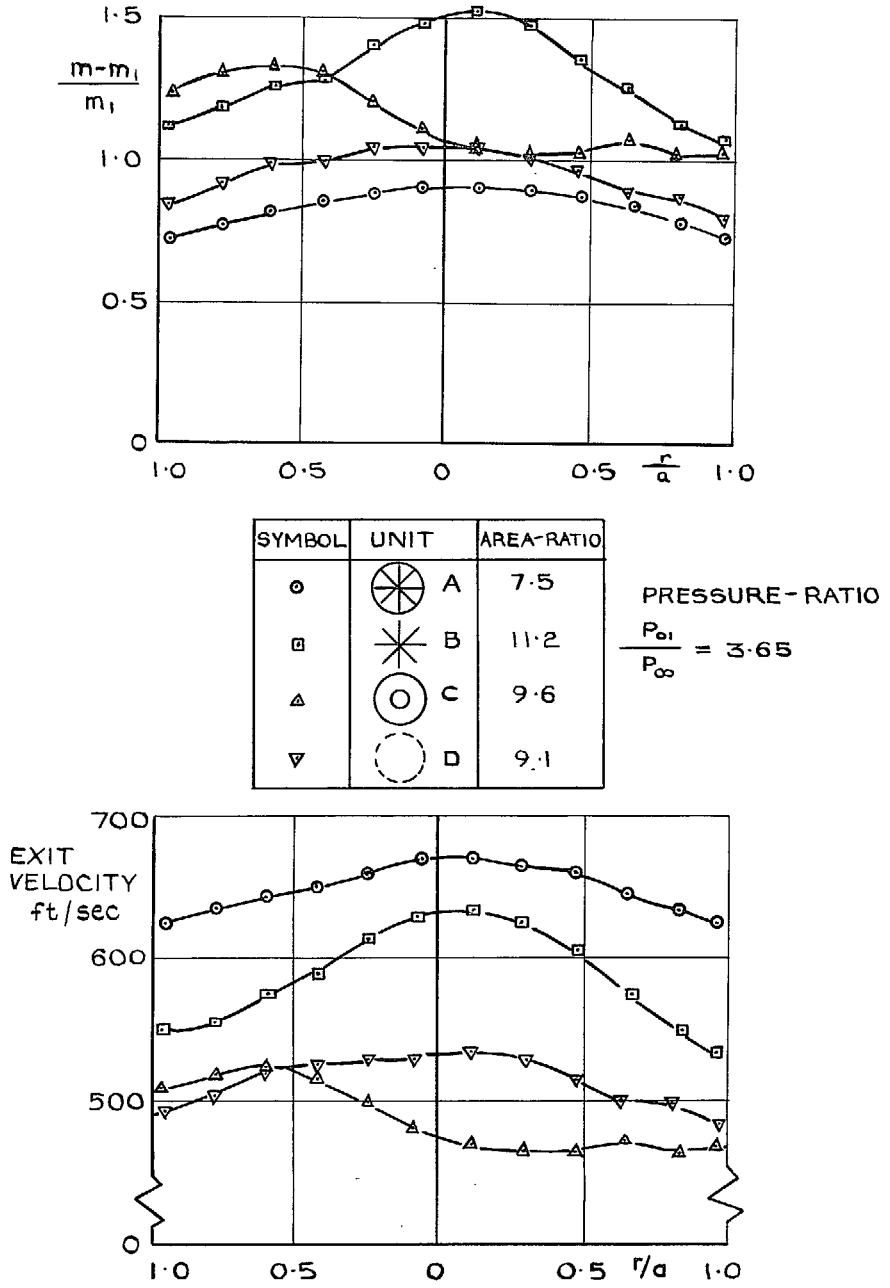


FIG. 3. Typical mass-ratio and velocity distributions at nozzle exit. Nozzle contraction ratio 1·45:1.

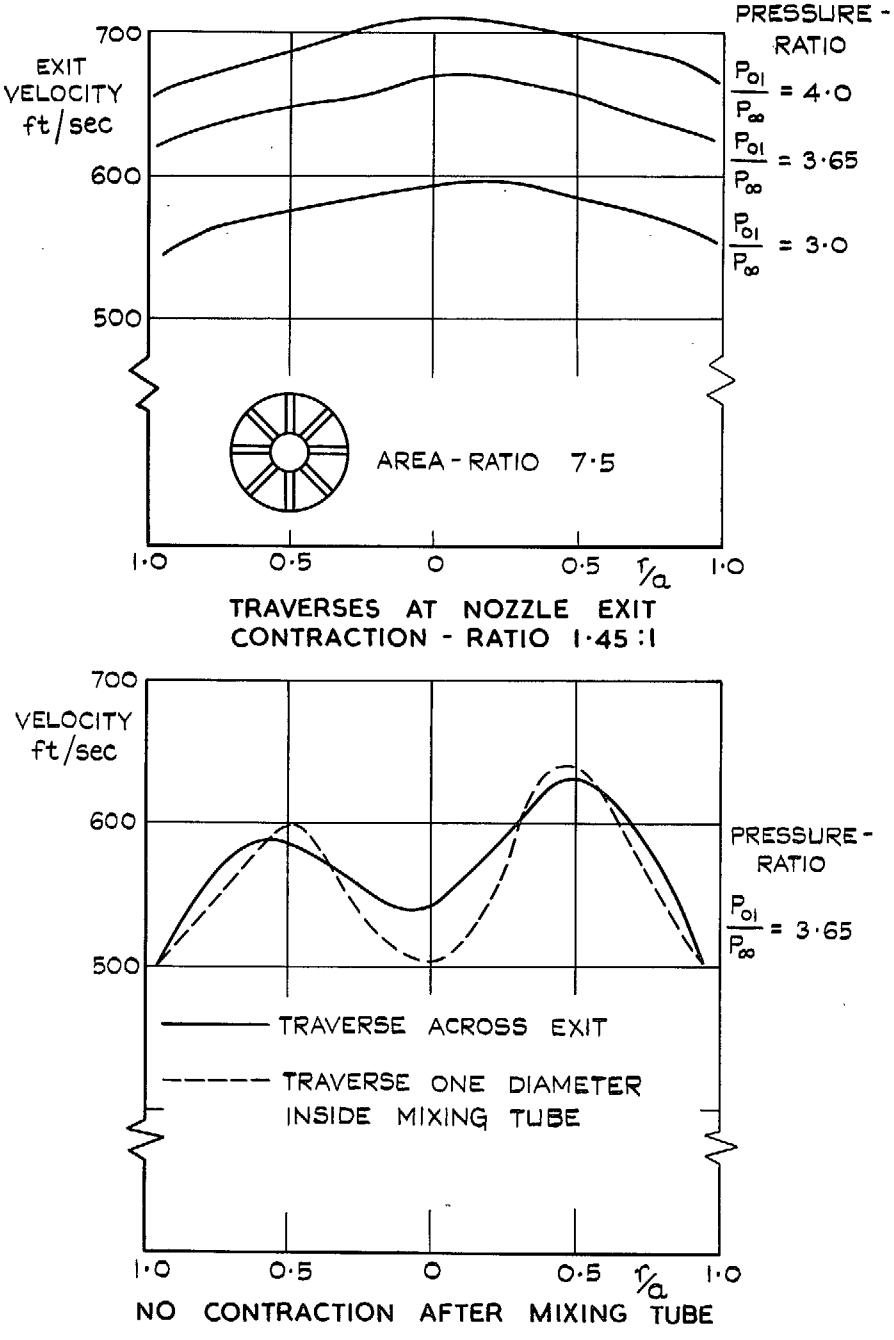


FIG. 4. Typical velocity distributions with 'cartwheel' injector unit.

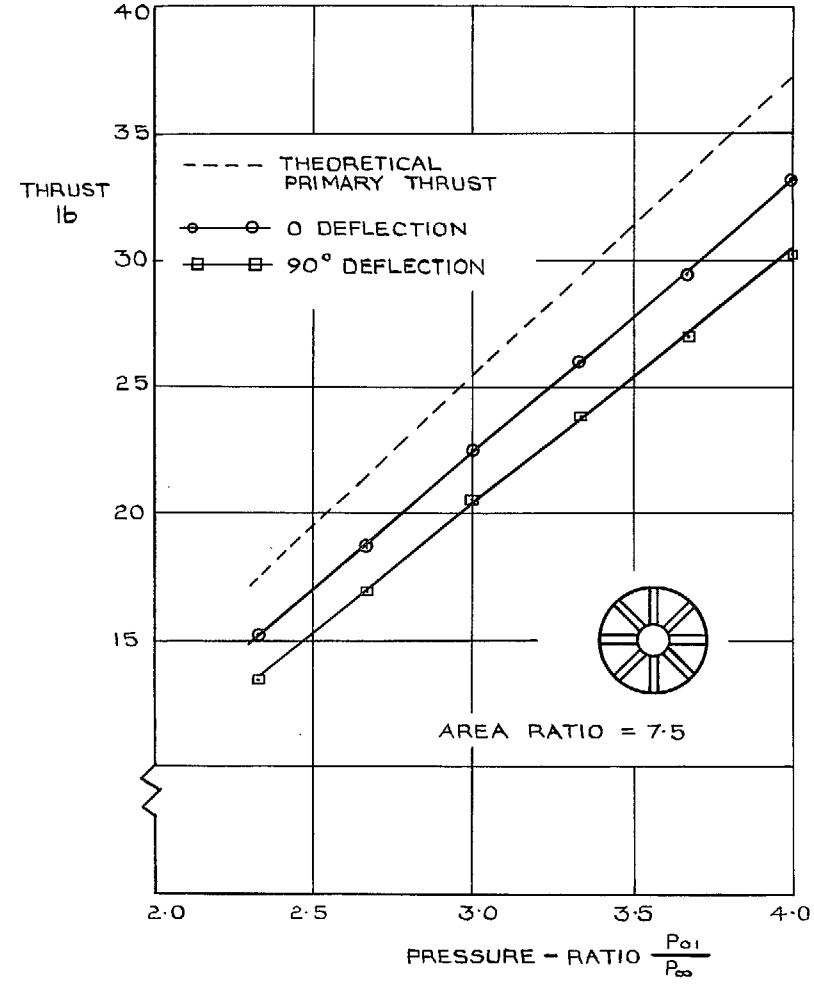


FIG. 5. Static thrust calibration

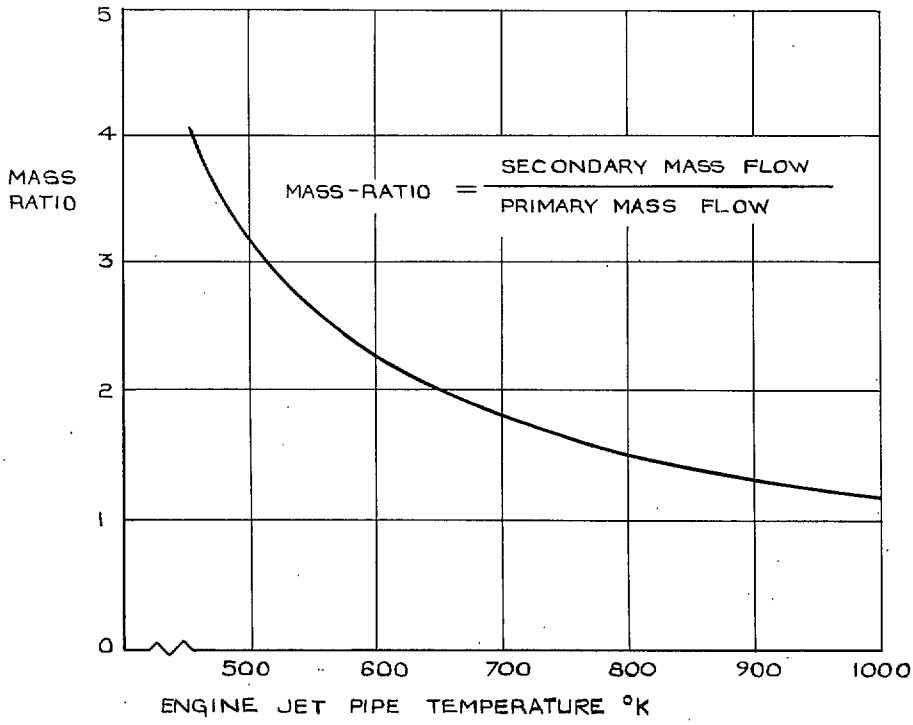


FIG. 6. Mass ratio required for engine simulation.

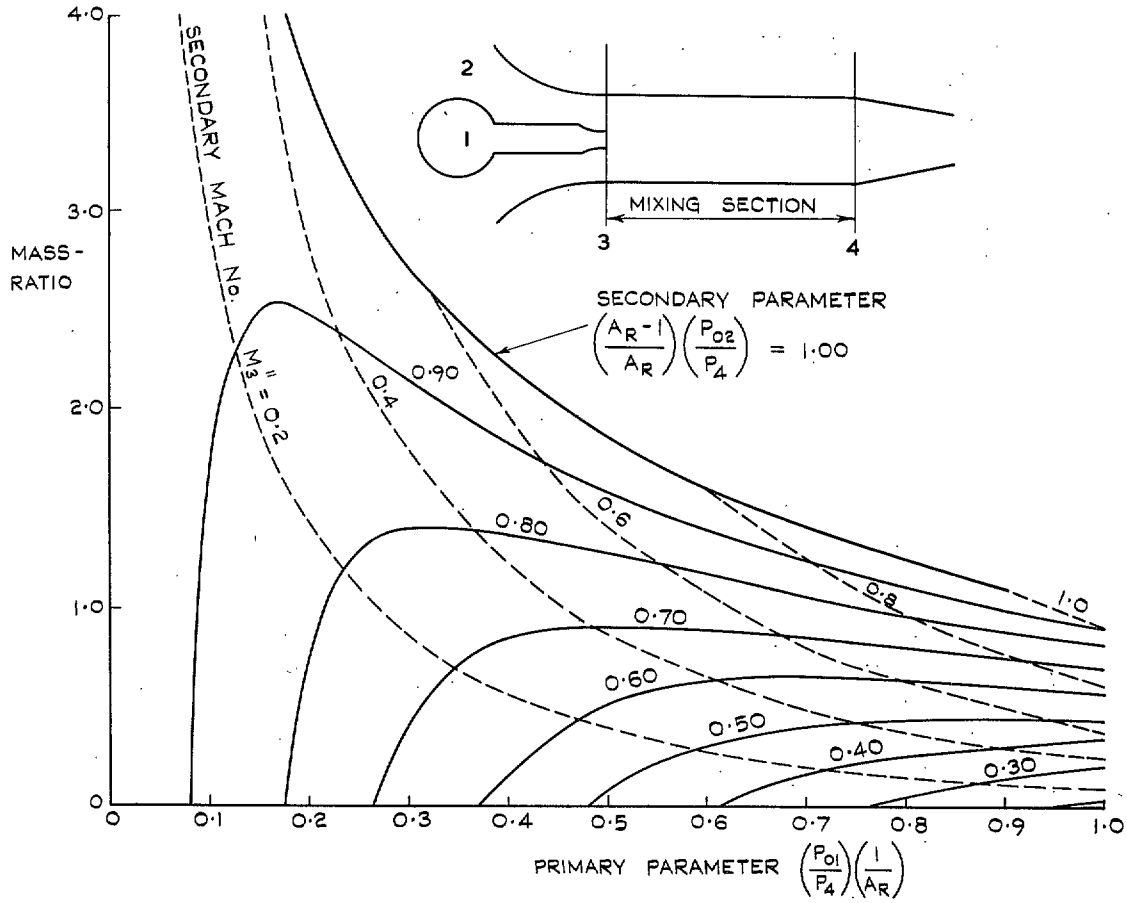


FIG. 7. Theoretical injector performance with sonic convergent primary nozzle.



Printed in Wales for Her Majesty's Stationery Office by Allens (Wales) Limited
Dd. 125874 K.5.

Published by
HER MAJESTY'S STATIONERY OFFICE

To be purchased from
49 High Holborn, London W.C.1
423 Oxford Street, London W.1
13A Castle Street, Edinburgh 2
109 St. Mary Street, Cardiff
Brazennose Street, Manchester 2
50 Fairfax Street, Bristol 1
35 Smallbrook, Ringway, Birmingham 5
7–11 Linenhall Street, Belfast 12
or through any bookseller



S.O. Code No. 23-3464